

RTG Radiator Efficiency in the Presence of Lunar Dust

M.M. Wittal¹, S.A. Miaule², M.A. Guerrero Nacif³, A.M. Swanger⁴, and J.G. Mantovani⁵

¹Robotics and Autonomous Systems Engineer, Granular Mechanics and Regolith Operations Laboratory & Deep Space Logistics, NASA Kennedy Space Center, FL, 32899 USA; email: matthew.m.wittal@nasa.gov

²Office of STEM Engagement Intern, NASA Kennedy Space Center, FL, 32899 USA

³Cryogenics Laboratory, NASA Kennedy Space Center, FL, 32899 USA

⁴Cryogenics Laboratory, NASA Kennedy Space Center, FL, 32899 USA

⁵Senior Physicist, Granular Mechanics and Regolith Operations Laboratory, NASA Kennedy Space Center, FL, 32899 USA

ABSTRACT

The accumulation of Lunar dust on various surfaces is the subject of much recent study, yet is still poorly understood. Recent plans to return humans to the Moon as part of the Artemis program mean that the presence of robust infrastructure to support a permanent human presence is inevitable. Power supply systems, such as Radioisotope Thermoelectric Generators are a likely part of that infrastructure, but require radiative thermal dissipation through a series of radiator fins to function effectively. In this work, the results of a parametric study of the impact on radiator efficiency due to various quantities and types of lunar dust simulants are presented, determining that the impact from low levels of lunar dust accumulation is not significantly detrimental to the efficiency of Multi-Mission Radioisotope Thermoelectric Generator performance in a vacuum, but increased fidelity of data would improve these findings..

INTRODUCTION

The hazards that lunar dust poses on the safety of astronauts and the reliability of equipment became evident during the Apollo program. Even during stays as short as a few days, the fine particles of lunar regolith became more than a mere nuisance. After decades of study, we now have a better idea of dust properties and behavior than ever before, yet there still remains many unknowns when it comes to what impact that dust may have on systems during long-term stays on or colonization of the Moon. One of those unknowns is how accumulated lunar dust effects the efficiency of radiative heat dissipation for an Radioisotope Thermoelectric Generator (RTG). The interior of Multi-Mission RTGs (MMRTGs) reach up to 510°K, and must be cooled in order to function properly. RTGs that have been used in the past have either been used in clean, dust-free environments, such as the vacuum of space, or in dusty, atmospheric environments such as Mars. In the former case, the determination of radiator efficiency becomes one of simple radiative heat transfer. In the latter, a combination of convection and radiation plays into the efficiency of the RTG, even when covered with dust. However, on the Moon or other small, dusty bodies with no atmosphere, it is unknown if the dust will significantly impact radiator performance. As seen in the past with the thermal modeling of emissivity on AZ-93 and AgFEP thermal control coatings, by varying the surface coverage of the samples with lunar simulant JSC-1AF. Both surfaces showed different emittance trends, one increasing and the other decreasing relative to the fractional coverage of dust over the surface [7], suggesting the importance of understanding dust accumulation and its effects on thermal radiation with different material surfaces. Thus, this work seeks to gain an understanding of what one might expect during the Artemis program and beyond.

BACKGROUND

Using dust samples from the lunar surface during testing, known henceforth as regolith, is impractical primarily due to the limited supply. Thus, most experiments use one of many regolith

simulants developed based on the properties of Lunar regolith. It is worth discussing the differences between regolith simulants and lunar regolith itself for the purposes of understanding the expected level of precision of the experiment campaign described in this work. Lunar regolith itself is not exposed to the daily erosion and oxidation environment that we take for granted here on Earth. Thus, when observed under a high level of magnification, even particles on the order of a few micrometers are still rough and jagged, which contributes to their adhesive and abrasive behavior. Simulants developed on Earth necessarily have different properties and are less abrasive when compared to their lunar counterparts.

The state-of-the-art of plume-surface interactions on extraterrestrial bodies - namely the Moon and Mars - is a rapidly evolving field based on the findings of the Apollo program and spurred on by recent ambitions to return to the Moon through the Artemis program as well as several independent endeavors aimed at Martian colonization. These efforts are not identical in their approach or objectives, but all share a need to understand and plan for the adhesion and ablation of surfaces due to the impact of fine particles generated by rocket plumes near the surface of foreign bodies. Not only does this dust post a hazard to human health and performance, but high-velocity dust may cause damage to nearby systems, fine particles may obstruct nominal operation of moving parts, and the electrostatic and adhesive properties of the dust may impede thermal management systems.

Fine particles on Earth, the Moon, and Mars are all distinct from one another in fundamental ways, however the properties of the latter two in their natural environments may produce counter-intuitive behavior to untrained observers. Lunar regolith consists of particles of the same size we would find on Earth all the way down to sub-micron particles. Unlike regolith on Earth, these particles are not eroded by wind or water and are thus far more abrasive, clinging to materials and even the inside of the lungs of astronauts. It has been known to interfere with mechanical processes and, due to the lower gravity, the kinetic behavior of these particles is greatly influenced by the local charged environment to a greater degree than gravity, causing 'lofting' of particles near the lunar surface [14]. The lack of any significant atmosphere on the lunar surface also means that lunar dust can be ejected from plume impingement or impact sites at extremely high velocities [4].

Dust contamination during the Apollo program was a notorious problem, even during the short visits to the lunar surface, totalling no longer than 75 hours at most. What is of most interest to this study is the understanding of dust generated at landing (Fig. 1), which generated craters underneath the lunar module and ejected particles at high speeds in all directions. Since Apollo, the dust trajectories and behavior has been extensively studied based almost exclusively on video recordings during those missions [9]. One other example of how this dust can impact other surface assets is Apollo 12, where the crew landed in close proximity (~ 155 m) to the Surveyor 3 probe. The mirror on that spacecraft was returned for detailed analysis and both the accumulation of dust and the pitting due to the Apollo 12 landing was measured, showing $101 \frac{\text{pits}}{\text{cm}^2}$ [6]. This provides a single data point in lunar dust ablation and adherence. However, Surveyor 3 itself was not in direct line of sight to the Lunar Lander, being partly sheltered by the rim of the crater. This means that our only experimental evidence of the ablative nature of lunar dust from the lunar surface is not a reliable one.

Artemis provides us with the opportunity to implement lessons through the experience gained from Apollo and then expand upon them with new research and applied technologies. Recent developments in the field of Computational Fluid Dynamics (CFD) have greatly increased our abilities to understand plume-surface interactions [3, 10], and the study of regolith combined with the mapping of the lunar surface, based partially on the LRO demonstrate a greater understanding of the variables that exist on the Lunar surface. What this means is that we can combine experimental, simulated, and analytical models to generate a first pass at comprehensive plume-surface interactions [16, 12, 15].

The primary constraint placed on understanding the properties and behavior of Lunar regolith is the high expense of obtaining real samples and the difficulty of reproducing them on Earth. Dust on other celestial bodies is formed from the unique environments of those worlds, and factors on Earth such as humidity and erosion as well as the lack of suitable production methods mean that precisely replicating that regolith with current technology is challenging. Thus, modern experiments rely on regolith *simulants* which, depending on the precise simulant in question, seek

to mimic the properties of extraterrestrial dust such as grain size, density, albedo, adhesiveness, chemical composition, or dynamic properties. However, no simulant exists that adequately mimics all of these at once. It is important to note that the adhesive properties and electrostatic behavior of real regolith are the most difficult properties to reproduce, as the jagged, rough particles cannot be duplicated precisely on Earth and the dynamic, charged environment is likewise often neutralized by Earth's relatively high atmospheric pressure.

Granular Mechanics

Granular mechanics is a field of physics which seeks to understand the aforementioned dynamics of fine dust particles. These dynamics may simply be the kinematics of high velocity particles explored by [12,15, 1], or lower-speed particle-particle interactions explored by [10] and [13]. Recent work in this field has investigated the possibility that dust generated by impacts or landings will accumulate in the Cislunar space [16] or even impact the Deep Space Gateway [12], but has come to a null conclusion. However, that isn't to say that risk from high-velocity particles don't exist. Indeed, for any human landing, the entire Lunar surface might expect to receive some impacts, with the frequency of impacts falling off as a function of distance from the landing site and lander size [11,12,8].

Current work in the field of granular mechanics is focusing on the study of the plume-surface interactions and the development of tools to better quantify the effects, quantity, velocities, and trajectories of the particles generated during a landing. Most of the modeling and prediction, to date, is based on a combination of Apollo video footage [9], extrapolation based on crude measurements of crater sizes under the lander [8], and analytical methods based on a combination of observations of cratering and CFD simulations [12], which will be discussed below. Instrumentation bound for the Moon, in the form of science payloads, must be developed as the Artemis program ramps up, yet designing an instrument robust enough to withstand the high-velocity impacts yet sensitive enough to take precise measurements is not an easy feat.

Charged particle interactions also play a significant role in modeling and understanding the

behavior of regolith on the surface of bodies with negligible atmospheres, such as the Moon. This plays a specific role in understanding the adhesiveness of fine particles, which may play a role in the thermal systems of spacecraft and, of specific interest for this study, the thermal efficiency of propulsion systems [2]. A layer of insulating material on a turbopump, for example, may inhibit nominal operation, and the charge buildup of reusable rocket components due to friction alone may induce failures that would not be present on Earth or in a vacuum-induced environment.

In the lunar environment, the fine particles in the regolith are usually more strongly influenced by electric fields than they are lunar gravity, itself being only 16.5% as strong as Earth's [5]. This is especially true of particles moving at high velocity moving through the magnetic fields Earth and the Sun, as demonstrated simply by Lorentz force. As velocity increases to the order of km/s so too does the Lorentz force, thus significantly overcoming the force of gravity for small particles. The presence of moisture also changes the precise behavior of these particles, affecting both their adhesion and charge. Furthermore, the gravity of Earth is, of course, vastly different than that of the Moon. On the Moon, charged particle dynamics are often far more dominant than gravitational charge. Thus, for a notional vertically-oriented plate such as what one would find on an RTG, regolith simulatant on Earth may fall off easily while it's counterpart on the Moon, exposed to real lunar regolith, may accumulate a large external layer of dust. During the 2005 Lunar Regolith Simulant Materials Workshop, it was addressed that the thermal radiator aboard the Apollo Lunar Roving Vehicle had to constantly be brushed off due to its accumulation of lunar dust, occupying valuable crew time. [2].

METHODOLOGY

In this section, the theory and methodology employed in the acquisition of the thermal properties of the regolith samples considered as well as that used for the experiment to determine the impact of dust adhesion to radiator fins on the efficiency of MMRTGs is expanded upon. Conclusions will be reserved for the following section.

Theory

The power emitted by a body in a vacuum follow an emission pattern in accordance with Stefan-Boltzman law such that

$$\dot{Q} = \dot{Q}_1 - \dot{Q}_2 \quad (1)$$

Where $\dot{Q} = A\sigma\epsilon T^4$ is the power in Watts, A is the area, σ is the Stephan-Boltzman constant, ϵ is the coefficient of emissivity that considers the object as a grey body instead of a black body, and T is the temperature in Kelvin. For specific configurations, we may add a coefficient, $F_{1 \rightarrow 2}$, that describes the relative surface areas known as the view factor. Adding this coefficient and substituting this into Eq. 1 above yields

$$\dot{Q} = A_1\sigma\epsilon F_{1 \rightarrow 2}(T_1^4 - T_2^4) \quad (2)$$

For surfaces with different emissivity coefficients, it can be shown that

$$\dot{Q} = \frac{\sigma(T_1^4 - T_2^4)}{\frac{1-\epsilon_1}{A_1\epsilon_1} + \frac{1}{A_1F_{1 \rightarrow 2}} + \frac{1-\epsilon_2}{A_2\epsilon_2}} \quad (3)$$

Four our specific configuration, we may consider two plane elements to the interior of a coaxial right circular cylinder (Fig. 3), one each for above and below the radiator fin. This can be expressed as

$$F_{1 \rightarrow 2} = \frac{1}{1 + R^2} - \frac{(1 - H)^2}{(1 - H)^2 + R^2} \quad (4)$$

where $H = \frac{h}{x}$ and $R = \frac{r}{x}$. If $h \geq x$, then this equation becomes

$$F_{1 \rightarrow 2} = \frac{1}{1 + R^2} \quad (5)$$

We must also consider the interaction between the fin and the top and bottom of the vacuum chamber, approximated as planar elements to circular discs in a parallel plane (Fig. 4), expressed

as:

$$F_{1 \rightarrow 2} = \frac{1}{H^2 + 1} \quad (6)$$

Now we have the rate of change of the energy in terms of Watts, but determine the temperature at any given time we must also understand the relation between energy in Joules and temperature in Kelvin. Thus, the specific heat of an object may be expressed as:

$$Q = mc\Delta T \quad (7)$$

Where m is the mass, and c is the coefficient of specific heats ($0.9 \frac{J}{g^\circ K}$ for aluminum 6063 and $0.5 \frac{J}{g^\circ K}$ for stainless steel). Rearranging Eq. 6, and summing \dot{Q} yields

$$\Delta T = \frac{\sum_{i=1}^N \dot{Q}_i dt}{mc} \quad (8)$$

Where N is the number of surface features being considered, in this case 4.

Thermal Properties Analysis

Four simulants, specifically the NU-LHT-2M, NU-LHT-4M, OPRH4W30, and LHS-1 simulants, developed by the University of Central Florida (UCF), were tested and compared against one another in terms of effective thermal conductivity, hereafter denoted by k . To do this, two tools were used: the C-Therm thermal profiling tool and the Macroflash tool.

C-Therm testing involved placing a known quantity of material into a metallic bin and taking many (~ 25) samples across a very small temperature gradient ($1.3^\circ K$) with each test taking place over ~ 1 minute. The advantages of this testing were the rapid turnaround and ease of access, but the disadvantage was that small changes in the environment, the simulant density or quantity, or test configuration seemed to produce significantly different readings. Although runs themselves were consistent from test-to-test, mean measurements from run-to-run displayed unsatisfactory variability.

The Macroflash tool instead used a known quantity of material spread across a relatively large area (76 mm) at a depth of between 3 and 6 mm, a large temperature gradient ($\sim 200^\circ$ K), and collected over a period of ~ 15 minutes. This larger gradient, area, and sample time sparks a greater confidence in the results produced by the Macroflash tool which, as seen in Fig. 2, show a significantly lower measurement than the estimates provided by the C-Therm tool. Additionally, all of the estimates produced by the Macroflash agree with measurements taken in 2019 of the JSC-1A simulant at ambient pressure ($0.0482 \frac{W}{m \cdot K}$) well within an order of magnitude.

These estimates were collected with the hope that they will provide some tools for modeling dust accumulation on various surfaces later during the analysis of the radiator fin efficiency experiment campaign and future work described in § 6.

Radiator Fin Efficiency Experiment

Radiator fins used on MMRTGs consist of 6063 aluminum mounted radially and parallel to the containment cylinder. For this experimental campaign, a single fin was manufactured and mounted to a block of 6061 aluminum, which simulated the casing, inside of which a 120V insertion heater was installed. The fin itself measures 11.5×11.5 cm in area, and 1.9 cm in thickness. Thermocouples were installed in the casing and in three locations along the radiator fin as illustrated in Fig. 5. The assembled apparatus was then placed inside of a vacuum chamber and horizontal to floor on a stainless steel rod and isolated from the walls. The vacuum chamber was then pumped down to the order of 0.04 Pa. The heater was likewise engaged and brought to a temperature of 510° K at which point the temperature along the length of the radiator was permitted to reach a steady-stated distribution. The heater was then disengaged and the fin was permitted to cool down for a period of 30 minutes.

After the radiator fin reached a steady-state (that is, temperatures were not rising or falling significantly along the length of the fin) the heater was turned off and the temperatures were monitored over a period of 30 minutes. After initial configuration was complete, tested, and any issues were troubleshooted, a series of control measurements could be taken. 3 trials were run

during which the radiator fin was not exposed to any simulant, allowing for a baseline measurement of efficiency to be collected. Those three runs were averaged together, serving as a control for the following trials. The results of this control run were plotted as a function of time in (Fig. 6).

Following this, the test was then repeated with increasing amounts (1g, 2.5g, 5g, and 7.5g) of various regolith simulants on top of the radiator in an attempt to observe the relative change in radiative efficiency. Like the control test, each test was repeated 3 times and the results were averaged together to help filter out any noise between runs. An example what a plot like this looks like can be seen in Fig. 7, where the line styles represent different dust loads and the colors represent thermocouple measurement locations. The thermocouples near the end of the radiator (thermocouples 3 and 4) began to sag somewhere along the testing, producing slightly erroneous readings for fin temperatures (See Fig 7). However, these problems did not impact final results, which were examining how heat dissipated from the simulated MMRTG chamber (thermocouple 1).

RESULTS

Results can be seen in Fig. 8. The data shows that low amounts of dust ($m < 0.10 \frac{\text{kg}}{\text{m}^2}$) does not effect radiator efficiency when compared with the untreated aluminum surface. This benefit is lost as the dust load increases and approaches $1 \frac{\text{kg}}{\text{m}^2}$, but large error bars due to variability from one trial to another make this uncertain. It is possible that the configuration changed unintentionally from one trial to another in the form of variable dust sample density and particle size, or differences in the way the dust was added to the fin's surface, and thus additional data or a new method for adding the dust may improve the results in the future.

There remain some concerns with this configuration that can potentially be rectified during future testing, specifically the reliability of the thermocouples, and the grain size of the regolith to which the radiator fins were exposed. Although a larger range of grain sizes could notionally clink to radiator fins, it is likely that only the finer particles would be kicked up during daily lunar surface activity and distant landings. Thus, the use of large-grain simulants, such as LHT-1 and OPRH4W30 are unlikely to present a realistic profile of the type of lunar dust that would impact

MMRTG radiators. Conclusions about grain size and regolith type are difficult to draw due to large error bars and high variability. However, there seems to be difference in the mass of accumulated dust itself. In Fig. 8, it can be seen that for dust loads of $0.075 \frac{\text{kg}}{\text{m}^2}$, $0.189 \frac{\text{kg}}{\text{m}^2}$, $0.378 \frac{\text{kg}}{\text{m}^2}$ and $0.567 \frac{\text{kg}}{\text{m}^2}$, the temperature dissipation during a 30-minute time period at a pressure of no more than 4 Pa, efficiency falls by around 10 degrees in each case.

CONCLUSION

This study shows that radiators exposed to low levels of lunar dust ($< 100 \frac{\text{g}}{\text{m}^2}$) do not experience any significant reduction in terms of efficiency Fig. 4. Large error bars despite taking as many as 9 samples demonstrates that there is a larger than ideal amount of variability in this testing configuration. Higher fidelity testing would improve the results and allow for a greater understanding of the impact of high levels of dust accumulation on RTGs. Even so, low levels of dust accumulation have lower error bars and show that, for the levels of dust contamination that would be expected, there is no significant detriment on performance for an MMRTG.

Future testing could be improved by finding a better way to distribute the dust across the surface of the radiator fin. It is hypothesized that variability in regolith density, particle size, and human error in distributing across the surface of the fin by hand all played a part in the large error bars as the mass of dust increases. It is worth noting that on a casing with 8 fins, the decreased performance, if it exists, would rise considerably for high dust loads.

However, it is clear that coatings that seek to maximize performance of radiators in a vacuum, such as the Solar White coating, would not be effective when exposed to dust and thus would not be worth the investment.

FUTURE WORK

Immediate future work aims to examine the steady-state measurements of the temperature along the length of the radiator fin and then examine how this compares to existing computational models when burdened with uniform layers of dust with the properties derived during the thermal characterization experiments described in § 3.

This test campaign also paves the way for a more sensitive analysis of dust on radiators for pressurized volumes such as lunar habitats or Gateway elements, where the differential temperature is more sensitive to change and lower temperature differentials between ambient and the volume in question is expected.

REFERENCES

Batcheldor, D., Mantovani, J., and Wittal, M. M. (2021). “Lunar regolith trajectories as a result of plume surface interactions.” *AAS Division of Planetary Science meeting #53*, Vol. 53.

Gaier, J. R. and Jaworskes, D. A. (2007, doi: 10.1063/1.2437437). “Lunar dust on heat rejection system surfaces: Problems and prospects.” *AIP Conference Proceedings*, Vol. 880.

Gale, M., Mehta, R. S., Liever, P., Curtis, J., and Yang, J. (2020, doi: 10.2514/6.2020-0797). “Realistic regolith models for plume-surface interaction in spacecraft propulsive landings.” *AIAA Scitech 2020 Forum*, number 0797.

Gladstone, G., Hurley, D., Rutherford, K., et al. (2010, doi:10.1126/science.1186474). “Lro-lamp observations of the Icross impact plume.” *Science*, 330, 472–476.

III, J. R. P., Wang, H., Hillegass, A., Esparza, A., Dove, A. R., and Elgohary, T. A. (2021). “Implementation of charged particle behavior in discrete element method (dem) simulations.” *ASCE Earth and Space Conference 2021*.

Immera, C., Metzger, P., Hintz, P., Nick, A., and Horan, R. (2011, doi: 10.1016/j.icarus.2010.11.013). “Apollo 12 lunar module exhaust plume impingement on lunar surveyor iii.” 211(2), 1089–1102.

J. Gaier, J. Siamidis, S. P. K. R. and Larkin, E. (2008). “The Effect of Simulated Lunar Dust on the Absorptivity, Emissivity, and Operating Temperature on AZ-93 and Ag/FEP Thermal Control Surfaces (December).

K.R. Housen, K. H. (2011, 10.1016/j.icarus.2010.09.017). “Ejecta from Impact Craters.” *Icarus*, 211, 856–875.

Lane, J. E. and Metzger, P. T. (2012). “Ballistics Model for Particles on a Horizontal Plane in a Vacuum Propelled by a Vertically Impinging Gas Jet.” *Particul. Sci. Tech.*, 30(2), 196–208.

Liever, P. A., Gale, M. P., Mehta, R. S., and Weaver, A. B. (2021). “Gas-particle flow simulations for martian and lunar plume-surface interaction prediction.” *Earth and Space 2021*.

Metzger, P. (2020). “Dust transport and its effects due to landing spacecraft.” *2020 Lunar Dust Workshop*.

M.M. Wittal, J.R. Phillips, P. M. et al..” *2020 AAS/AIAA Astrodynamics Specialist Conference*.

Mueller, R. P., Gelino, N. J., Dixon, K. L., Sibille, L., and Vu, B. T. (2021). “Large vehicle lunar landing surface interaction and in-situ resource based risk mitigation: Landing & launch pads.” *AIAA ASCEND 2021*, Vol. 2021-4071.

Orger, N. C., Rodrigo, J., Alarcon, C., Toyoda, K., and Cho, M. (2018, doi: 10.1016/j.asr.2018.05.027). “Lunar dust lofting due to surface electric field and charging within micro-cavities between dust grains above the terminator region.” *Advances in Space Research*, Vol. 64, 896–911.

Wittal, M. and Butts, S. (2021). “System-level model-based risk determination for lunar mission design.” *21st IAASS Conference*.

Wittal, M. and Powers, R. (2019). “Spaceflight hazards of escape-velocity-domain impact ejecta in the cr3bp.” *2019 AAS/AIAA Astrodynamics Specialist Conference*.

List of Figures

1	15
2	The results of measuring the thermal conductivity of each sample approximately 4 mm in thickness for various samples. The dashed lines denote the average for each trial run, but they are both very similar to one another and within the range expected and historical measurements of regolith simulants provided by Johnson Space Center. 16
3	The configuration of the mathematical model. 17
4	The configuration of the mathematical model. 18
5	The preliminary configuration of the testing apparatus for the radiator efficiency test. In the final configuration, the hemispheres were not employed as they were deemed unnecessary in the vacuum chamber, but future testing for smaller temperature ranges simulating pressurized habitats or elements as described in §6 may necessitate it's use. 19
6	The averaged results of 3 control trials measured at the casing and three locations along the radiator fin. 20
7	The averaged results of 3 control trials of the NU-LHT-2M simulant from UCF. The red, blue, green, and black line sets correspond to the casing, fin 1, fin 2, and fin 3 thermocouple locations. 21
8	The results of 3 averaged trials of 7 different regolith burdens for the NU-LHT-2M. The values of 0.5g, 1g, 1.5g, 2g, 2.5g, 5g, and 7.5g correspond to $0.038 \frac{\text{kg}}{\text{m}^2}$, $0.075 \frac{\text{kg}}{\text{m}^2}$, $0.113 \frac{\text{kg}}{\text{m}^2}$, $0.151 \frac{\text{kg}}{\text{m}^2}$, $0.189 \frac{\text{kg}}{\text{m}^2}$, $0.378 \frac{\text{kg}}{\text{m}^2}$, and $0.567 \frac{\text{kg}}{\text{m}^2}$, respectively. Also plotted are the different regolith simulant burdens for the NU-LHT-4M, the OPRH4W30, and LHS-1, but these plots only include the values of 1g, 2.5g, 5g, and 7.5g due to time constraints. Future work intends to further refine these data sets. 22

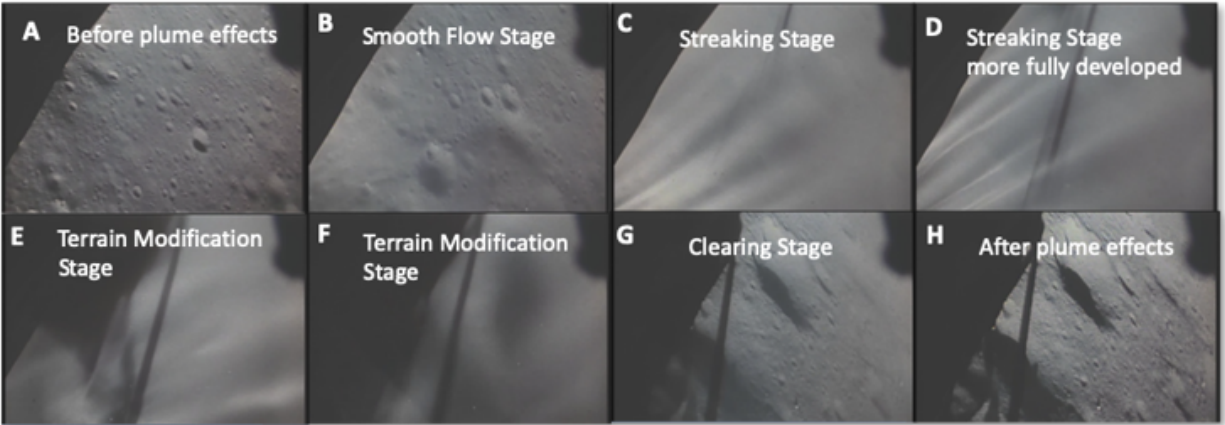


Fig. 1.

Clips from the Apollo 15 showing the large amounts of dust generated from the lander plume of the Lunar Descent Module. Image compiled by [11].

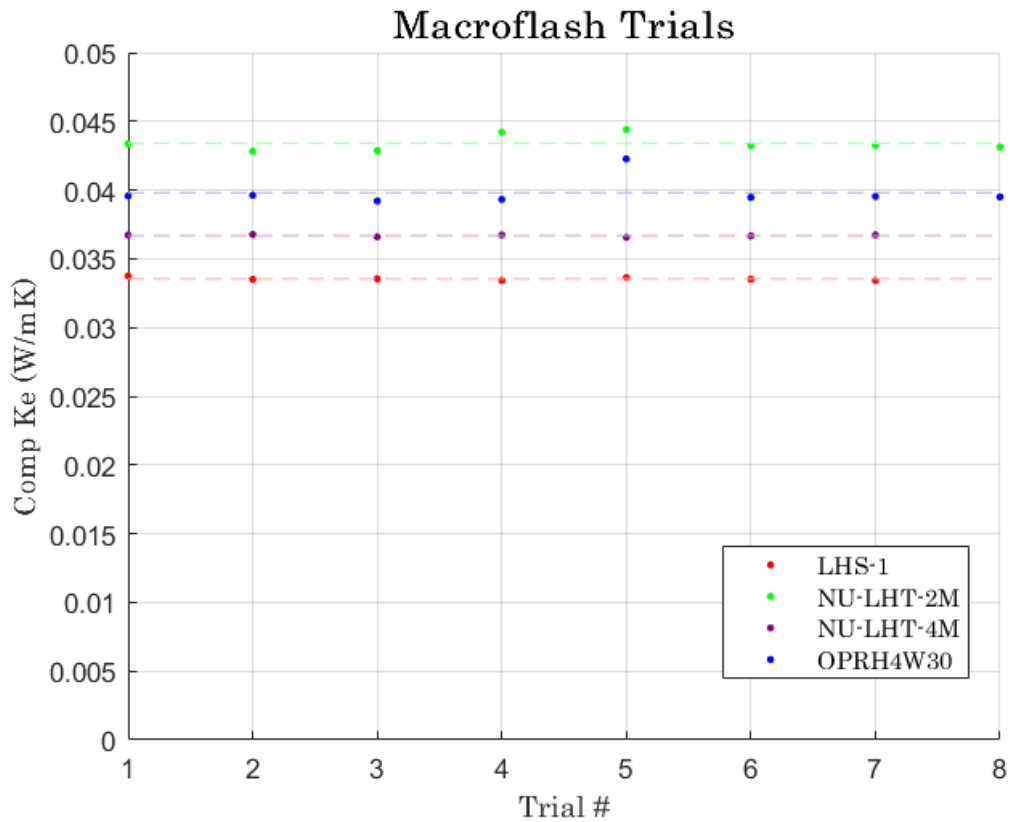


Fig. 2. The results of measuring the thermal conductivity of each sample approximately 4 mm in thickness for various samples. The dashed lines denote the average for each trial run, but they are both very similar to one another and within the range expected and historical measurements of regolith simulants provided by Johnson Space Center.

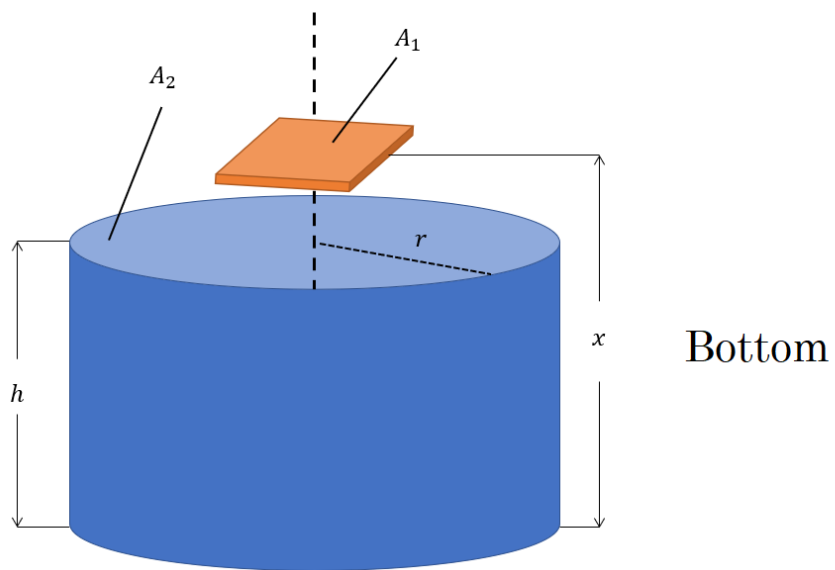
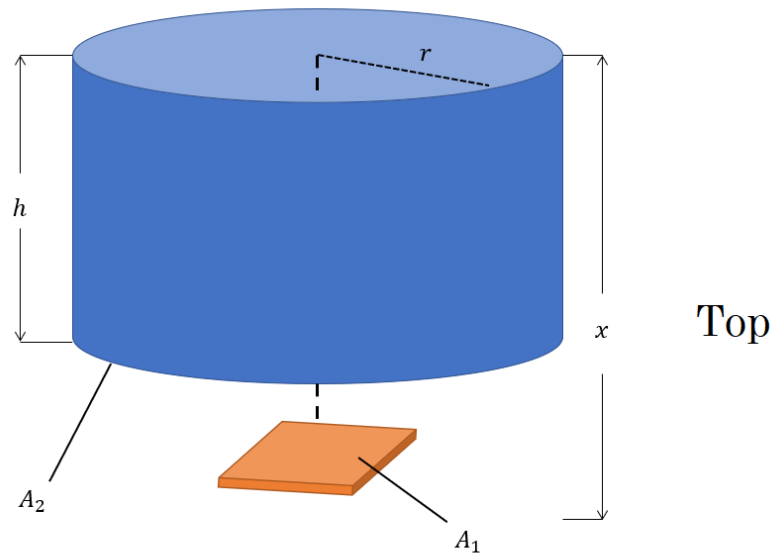


Fig. 3. The configuration of the mathematical model.

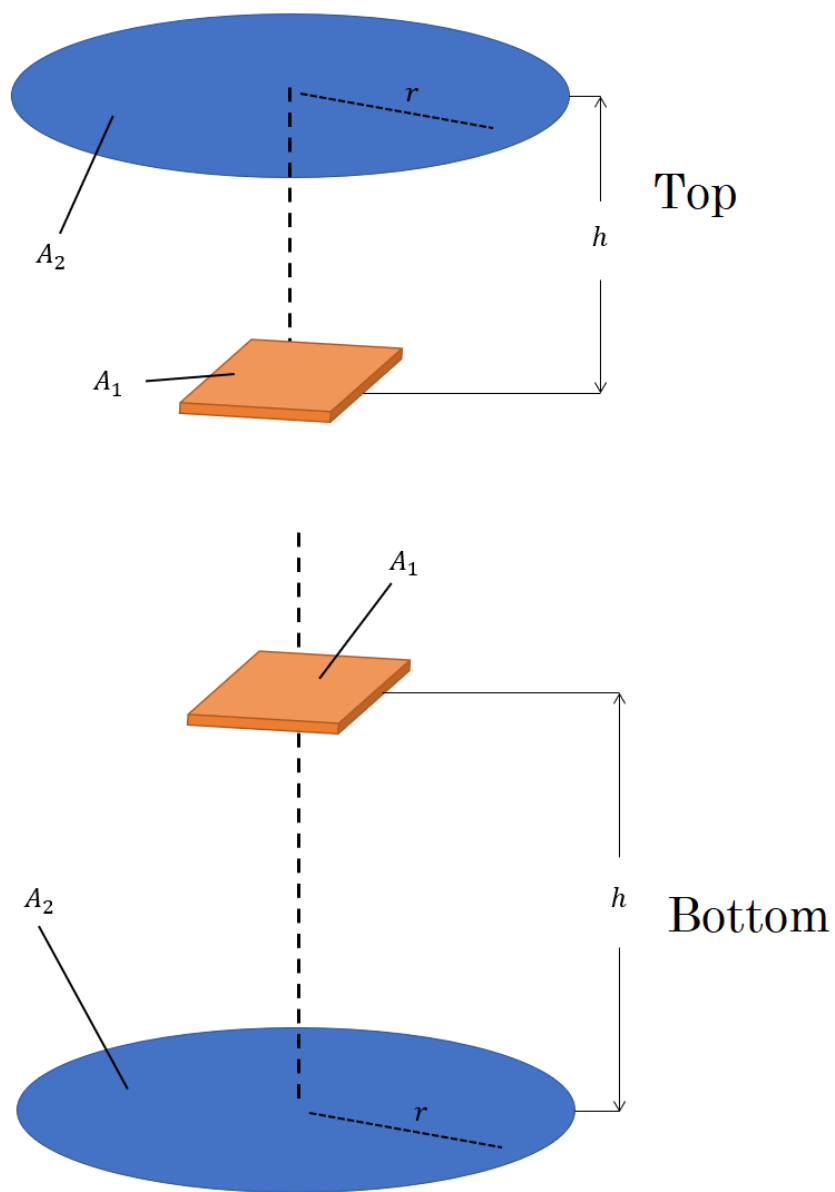


Fig. 4. The configuration of the mathematical model.

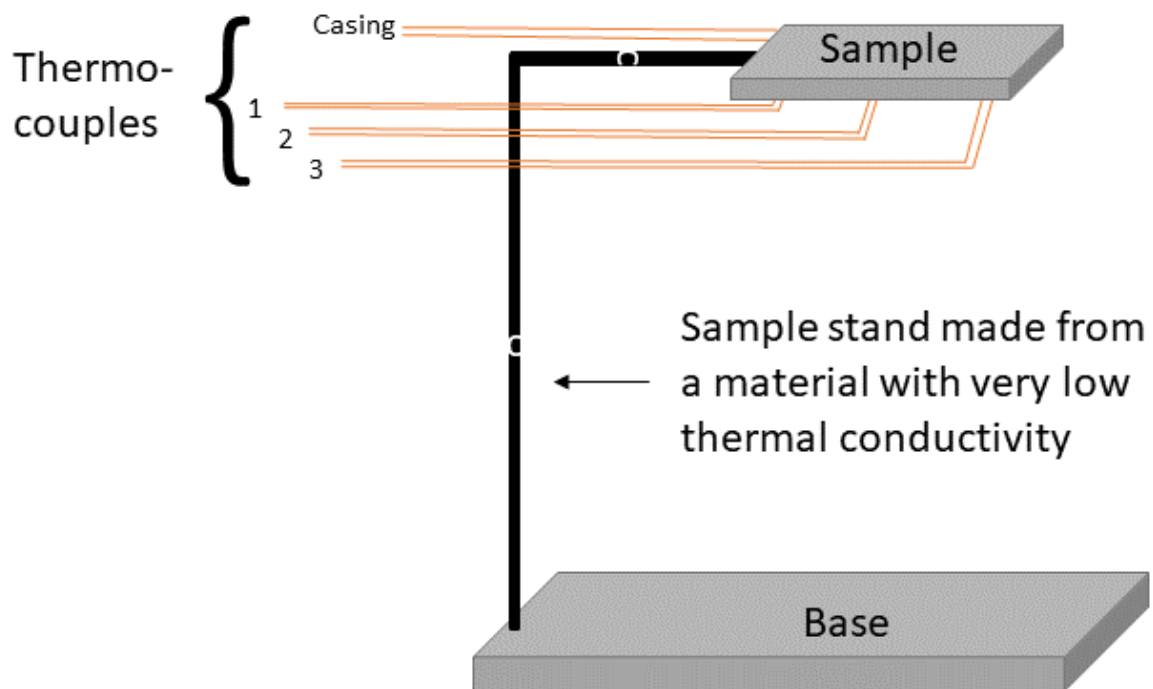


Fig. 5. The preliminary configuration of the testing apparatus for the radiator efficiency test. In the final configuration, the hemispheres were not employed as they were deemed unnecessary in the vacuum chamber, but future testing for smaller temperature ranges simulating pressurized habitats or elements as described in §6 may necessitate it's use.

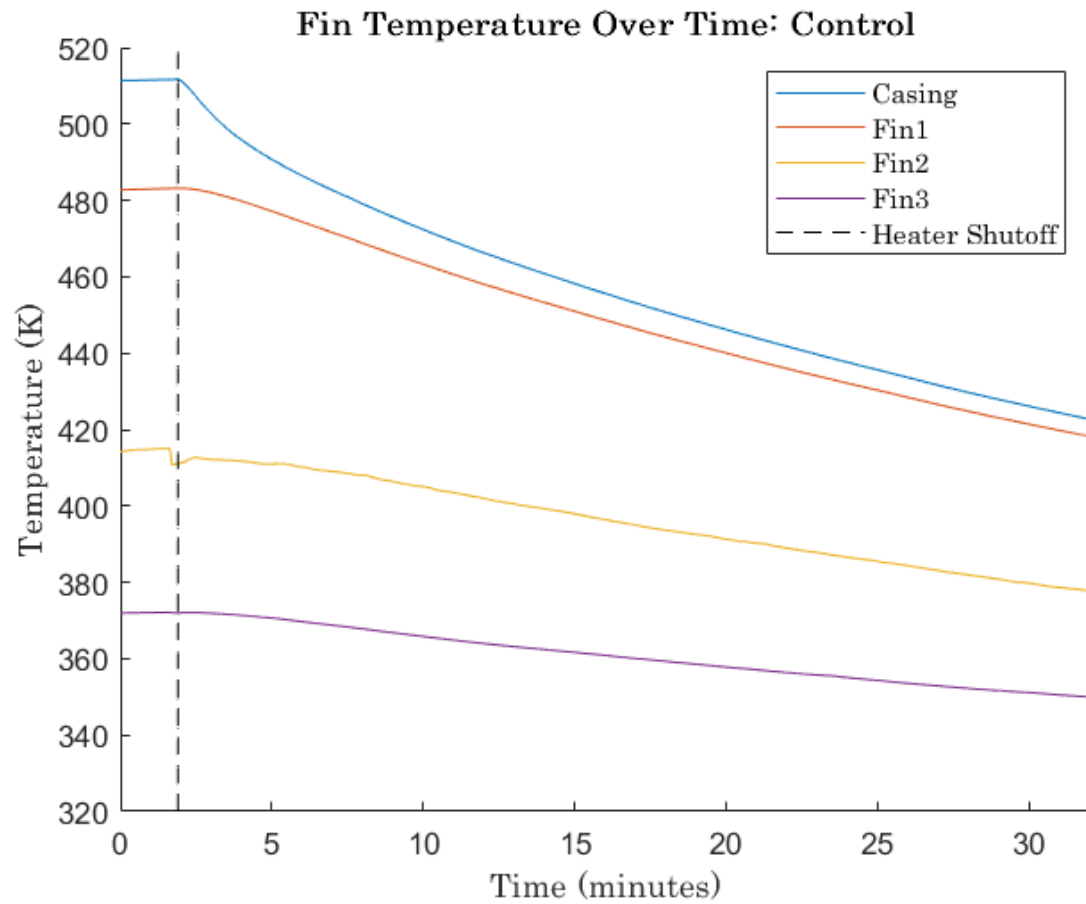


Fig. 6. The averaged results of 3 control trials measured at the casing and three locations along the radiator fin.

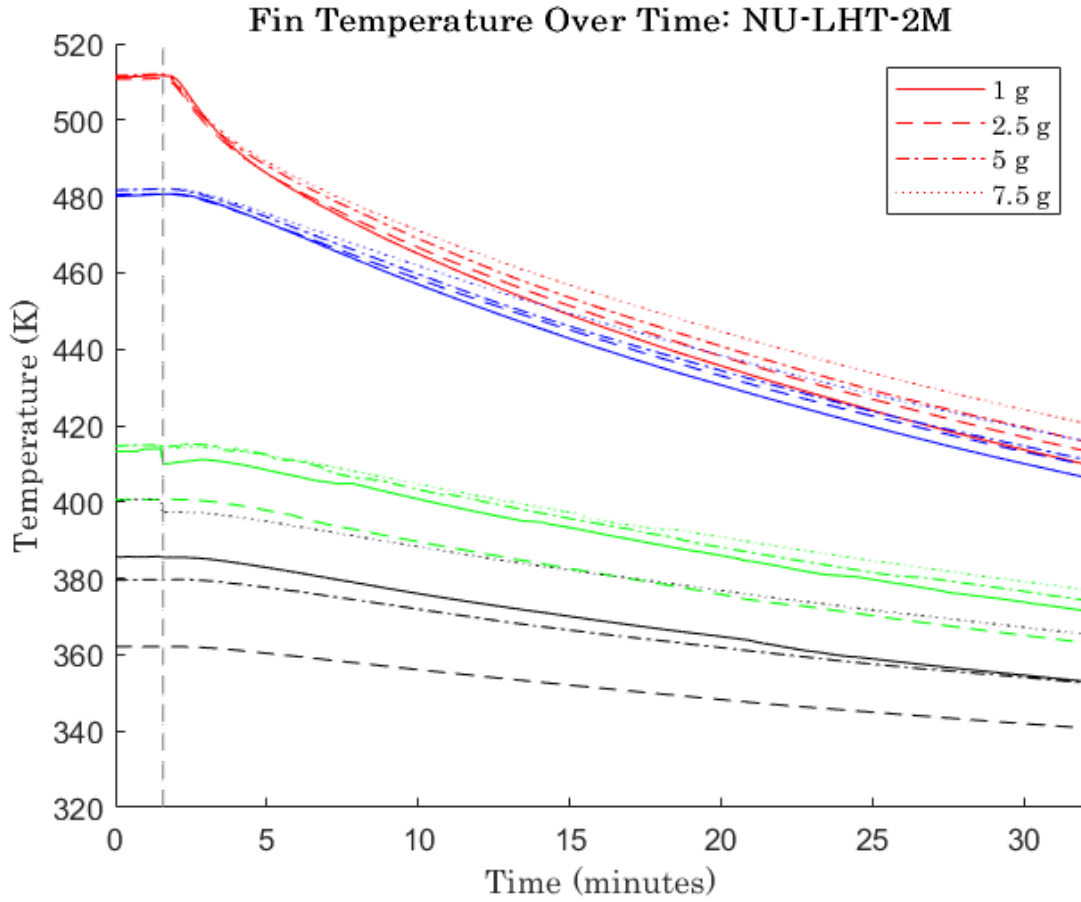


Fig. 7. The averaged results of 3 control trials of the NU-LHT-2M simulant from UCF. The red, blue, green, and black line sets correspond to the casing, fin 1, fin 2, and fin 3 thermocouple locations.

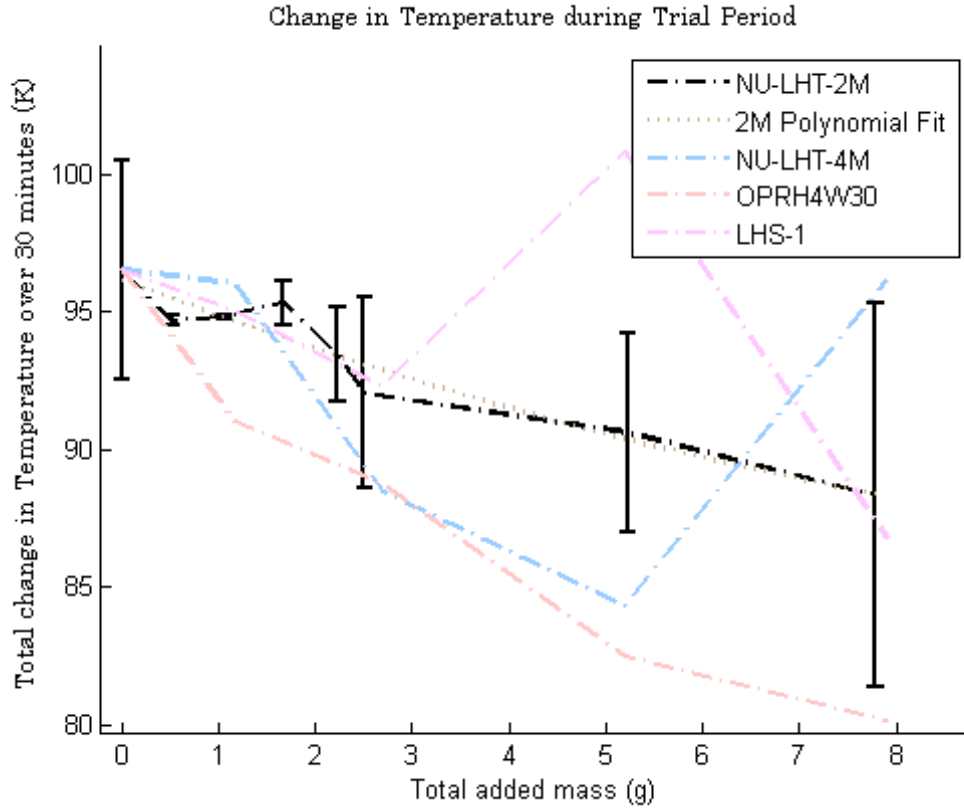


Fig. 8. The results of 3 averaged trials of 7 different regolith burdens for the NU-LHT-2M. The values of 0.5g, 1g, 1.5g, 2g, 2.5g, 5g, and 7.5g correspond to $0.038 \frac{\text{kg}}{\text{m}^2}$, $0.075 \frac{\text{kg}}{\text{m}^2}$, $0.113 \frac{\text{kg}}{\text{m}^2}$, $0.151 \frac{\text{kg}}{\text{m}^2}$, $0.189 \frac{\text{kg}}{\text{m}^2}$, $0.378 \frac{\text{kg}}{\text{m}^2}$, and $0.567 \frac{\text{kg}}{\text{m}^2}$, respectively. Also plotted are the different regolith simulant burdens for the NU-LHT-4M, the OPRH4W30, and LHS-1, but these plots only include the values of 1g, 2.5g, 5g, and 7.5g due to time constraints. Future work intends to further refine these data sets.